

Sabieh

2 Jan 2018

# Paramagnetic Leidenfrost drops under the influence of an inhomogeneous magnetic field

Shafia Elahi

Roll no: 2018-12-0005

LUMS School of Science and Engineering

Tuesday, January 1<sup>st</sup>, 2019

## 1 Abstract

We observe and record the trajectories of liquid oxygen drops in the Leidenfrost state under the influence of an inhomogeneous magnetic field. As oxygen is paramagnetic, we expect a deviation in its path. Using video motion analysis and computational tools, it is shown that the presence of the magnetic field changes the velocity of the drops, in both direction and magnitude. We explain this deviation in the drop's trajectory in terms of classical mechanics and compare the experimental results with our theoretical predictions.

## 2 Introduction

The paramagnetic behaviour of oxygen was discovered by James Dewar in the late 19<sup>th</sup> century who showed that liquid oxygen is attracted by the poles of an electromagnet [3]. In this experiment, liquid oxygen drops are obtained by means of condensation on the surface of a copper cone, that has been cooled down to  $-196^{\circ}\text{C}$  using liquid nitrogen. As the boiling point of oxygen is  $-183^{\circ}\text{C}$ , we see liquid droplets condense on the surface of the cone. At this temperature, other components of air that might be present in the liquid droplets are argon, which liquefies at  $-186^{\circ}\text{C}$ , water vapour in roughly around 5% and carbon dioxide making up roughly 1%. However, the paramagnetic nature of the drop observed is only due to oxygen. At room temperature which is significantly hotter than its boiling point, an oxygen drop on a substrate rapidly evaporates and as a result, is seen to hover over a thin film of insulating vapour, a phenomena known as the Leidenfrost effect. This remarkably reduces frictional effects on the drops due to which they are seen to maintain a rounded shape and constant velocity. Significant deceleration is not observed till the drop with an initial speed of a few tens of centimeters has traveled several meters [4].

In this article, we obtain a classical equation of motion for the drop by conservation of energy considerations. This allows us to predict the peripheral radius of the trajectory from the center of the magnet  $r_p$ , and its angle of deflection  $\alpha$ . We then compare the predicted values with the ones obtained experimentally. *quantification*

where is [1] & [2]?

(P)

NEW  
PARA

## 3 Theory

The molecular orbital theory explains the paramagnetism of oxygen [5]. As the oxygen molecule has two unpaired electrons, and each electron acts like a magnetic dipole due to its spin, in the presence of an external magnetic field these align in the direction of the applied magnetic field. Hence, a magnetic force is exerted on the oxygen drops.

The magnetic energy per unit volume in a region is defined as:

$$E_{mag} = \frac{|B|^2}{2\mu} \quad (1)$$

$$\mu = \mu_r \mu_0 \quad (2)$$

connection?

NOT NEEDED here

where  $\mathbf{B}$  is the magnetic field in the region and  $\mu$  the permeability, defined as the product of the relative permeability of the medium  $\mu_r$ , and of the permeability of free space  $\mu_0$ . The relation between the relative permeability of the material  $\mu_r$  and its volume magnetic susceptibility  $\chi$  is defined by,

*given*  $\mu_r = 1 + \chi$  *make a connection between equations*

$$\Rightarrow E_{mag} = \frac{|\mathbf{B}|^2}{2\mu_0(1 + \chi)} \quad (3)$$

*[ref. needed]*

At  $-183^\circ\text{C}$ ,  $\chi = 0.0035$  for oxygen. As  $\chi \ll 1$ , we expand (3) using binomial expansion up to  $O(\chi)$ ,

$$\frac{|\mathbf{B}|^2}{2\mu_0}(1 + \chi)^{-1} \approx \frac{|\mathbf{B}|^2}{2\mu_0} - \frac{\chi|\mathbf{B}|^2}{2\mu_0} \quad (4)$$

We can ignore the first term on the right hand side of (4) as it just represents the magnetic energy density in vacuum. The second term is the contribution to the magnetic energy from the paramagnetic substance. Hence, the magnet exerts an attractive force on liquid oxygen, which derives from the magnetic energy per unit volume:

$$E_{mag} = -\frac{\chi}{2\mu_0} B^2 \quad (5)$$

Using a Gaussmeter,  $B$  is measured and values for  $E_{mag}$  plotted against radial distance from the center of magnet.  $|E_{mag}|$  is greatest right above the magnet, whereas far from the magnet,  $B$  is classically found to vary  $\propto \frac{1}{r^3} \Rightarrow E_{mag} \propto \frac{1}{r^6}$ . Using these limiting relations,  $E_{mag}$  can be expressed as:

$$E_{mag} = -\frac{E_0}{q + (\frac{r}{r_0})^6} \quad (6)$$

where the constants  $E_0$ ,  $q$  and  $r_0$  are determined by least-square fitting  $E_{mag}$  found from measured values of  $B$ .

The drop has kinetic energy per unit volume,

$$E_{kinetic} = \frac{\rho \vec{v}^2}{2} \equiv \frac{1}{2} \rho (\dot{r}^2 + r^2 \dot{\theta}^2) \quad (7)$$

where  $\rho$  is the density of liquid oxygen, and  $v_i$  its velocity. The energy per unit volume is thus  $E_{mag} + E_{kinetic}$  that is equal to the initial kinetic energy of the drop (we ignore its gravitational potential energy as the drop moves on a horizontal plate),

$$\frac{1}{2} \rho \vec{V}^2 = \frac{1}{2} \rho (\dot{r}^2 + r^2 \dot{\theta}^2) - \frac{E_0}{q + \frac{r}{r_0}^6} \quad (8)$$

where  $\vec{V}$  is the initial velocity of the drop.

Our setup is invariant under rotation in the horizontal plane as we are using cylindrical magnets, hence angular momentum is conserved (see Fig. 1.),

$$\vec{L} = m|\vec{r}||\vec{V}| \sin \theta = m|\vec{r}| \sin \theta |\vec{V}| = mbV \quad (9)$$

where  $m$  is the mass of the drop. Along the trajectory, its angular momentum is,

$$\vec{L} \equiv m|\vec{r}||\vec{v}_{tangential}| \equiv mr(r\dot{\theta}) \equiv mr^2\dot{\theta} \quad (10)$$

← Equating (9) and (10),

$$r^2\dot{\theta} = bV \Rightarrow \dot{\theta} = \frac{bV}{r^2} \quad (11)$$

Substituting (11) in (8), we get our final form for the equation of motion of the drop:

$$\rho \frac{\dot{r}^2}{2} + E_{eff}(r) = \frac{\rho V^2}{2} \quad (12)$$

where  $E_{eff}(r) = \frac{\rho b^2 V^2}{2r^4} - \frac{E_0}{q + \frac{r}{r_0}^6} \equiv \frac{\rho b^2 V^2}{2r^4} + E_{mag}$ .

*use slanted fractions inline, e.g.  $\rho b^2 V^2 / 2 r^2$  etc.*



You need to define  $r_p$  first

At  $r_p$ ,

$$\dot{r} = 0 \implies E_{eff}(r) = \frac{\rho V^2}{2} \quad (13)$$

Hence, the intersection of  $E_{eff}$  and  $\frac{\rho V^2}{2}$  plotted against  $r$  correspond to  $r_p$ , for corresponding values of  $b$ .

The deflection  $\alpha$  can be calculated by integrating  $\dot{\theta}$  along the trajectory. From (11) and (12),

$$\begin{aligned} \dot{r} &= \frac{dr}{d\theta} \frac{d\theta}{dt} = \frac{bV}{r^2} \frac{dr}{d\theta} \implies \\ d\theta &= \frac{bdr}{r^2 \sqrt{1 - \frac{2E_{eff}}{\rho V^2}}} \implies \\ \theta &= \int_{r_p}^{\infty} \frac{dr}{r^2 \sqrt{1 - \frac{2E_{eff}(r)}{\rho V^2}}} \end{aligned}$$

Put more narration isted  
of putting one (14)  
equation after the other.

The angle of deflection is then (see Fig. 1),

$$\alpha = 2 \int_{r_p}^{\infty} \frac{dr}{r^2 \sqrt{1 - \frac{2E_{eff}(r)}{\rho V^2}}} - \pi \quad (15)$$

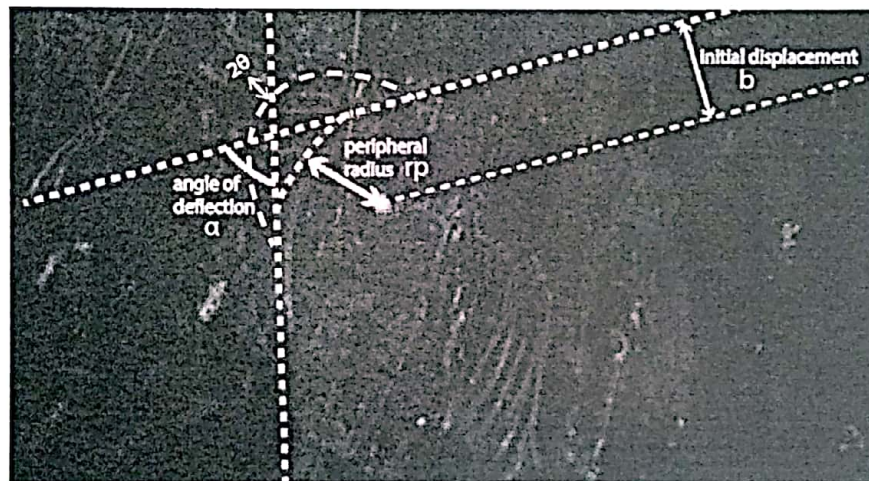


Figure 1: The angle of deflection  $\alpha$  and the peripheral radius  $r_p$  [1]

## 4 Experimental Setup



Figure 2: Experimental setup in lab [1]

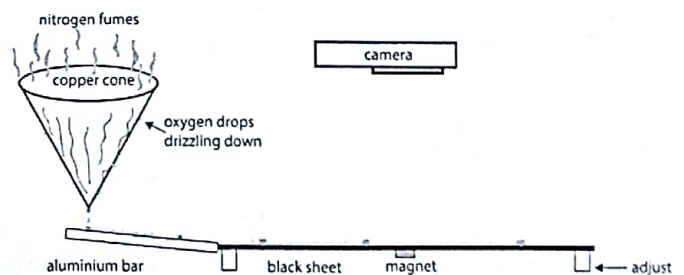


Figure 3: Simplified diagrammatical view of schematic [2]



The schematic of the apparatus is shown in Figure 2. A copper sheet is folded and welded to form a cone of about 10 cm in height and width. Liquid nitrogen is then poured into it, and the cone quickly reaches  $-196^\circ\text{C}$ . A film of liquid is seen collecting on its external surface which then collects at the tip forming a drop of typical radius 1 mm. The drop then drips into a depression that runs along the length of an aluminium bar placed under the cone. The bar rests on top of a triangular block support allowing its height above the table and inclination to be varied, that in turn varies the velocity of the incoming drop. The height of the cone can also be adjusted to vary the velocity.

The drop runs down the aluminium rod and onto a horizontal Plexiglas plate with a thickness of  $(3 \pm 0.5)$  mm, underneath which a cylindrical neodymium magnet (measuring 2 cm in diameter and 1.5 cm in height) is attached. The magnetic field is on the order of 0.223 T at the center and decreases on a distance comparable to its size.

Using a Gaussmeter,  $B$  was measured in the horizontal plane and values obtained for  $E_{mag}$  as a function of the radial coordinate ( $r$ ), with the origin of our coordinate system placed at the center of the magnet.

We measured the deflection  $\alpha$  and the distance  $r_p$  to the pericenter of the trajectory (where the radial velocity is equal to zero), as a function of  $b$  for  $V = (17 \pm 2)$  cm/s. This was done using video tracking software. The data obtained was then extracted to Matlab, and the quantities of interest obtained computationally.

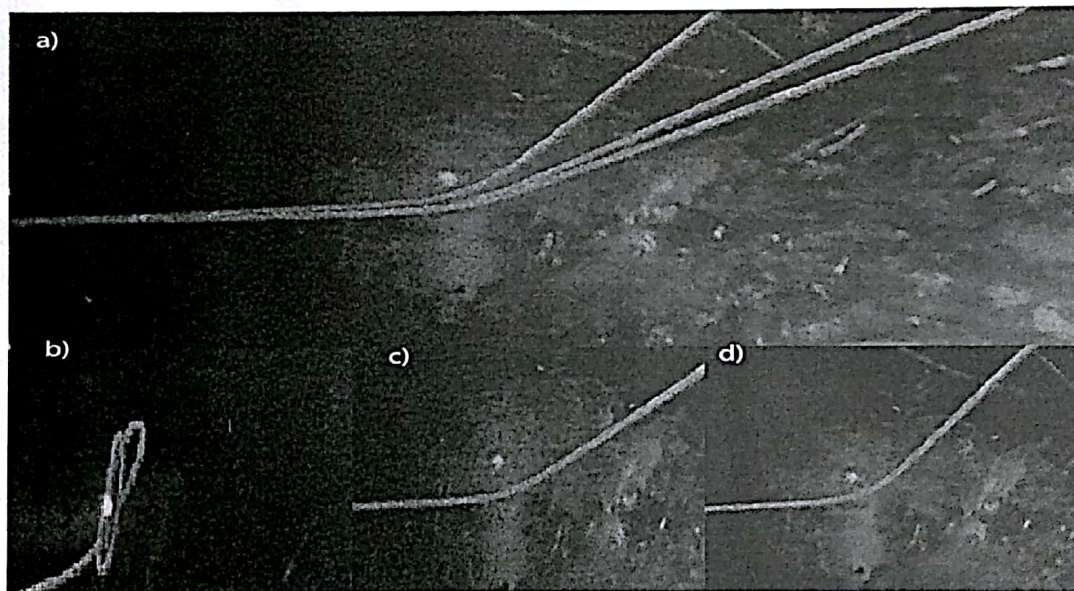


Figure 4: Top views of oxygen drop trajectories on a horizontal Plexiglas plate below which a magnet has been placed (its position marked with a white dot). Changing the impact parameter changes the amount of deflection. In b) ( $b \approx 8.7\text{mm}$ ,  $V = (17 \pm 2)$  cm/s) the drop is seen orbiting around the magnet.

— Also label the trajectories in (a), (c) & (d).  
What do the different subfigures represent?

## 5 Results and Discussion

Fig. 5 shows the values obtained for  $E_{mag}$  and its best fit, from which values for the constants  $E_0$ ,  $q$  and  $r_0$  were determined in Eq. (6).

Fig. 6 shows  $E_{eff}$  as a function of the radial distance from the center of the magnet, for different impact parameters  $b$ . On the same graph is plotted the initial kinetic energy for  $V = 17$  cm/s. The points of intersection of the two graphs give the predicted values for  $r_p$ .

The calculation of  $r_p$  from solving (13) was done numerically; for a range of values of  $b$ , points of intersection of the two curves on both sides of the equation were found on Matlab and  $r_p$  was extracted from the data for each value of  $b$ . This theoretical prediction for  $r_p$  is represented by the curve in Figure 7. The experimentally measured values of  $r_p$  using tracking software are shown on the same plot by circles.

which software?

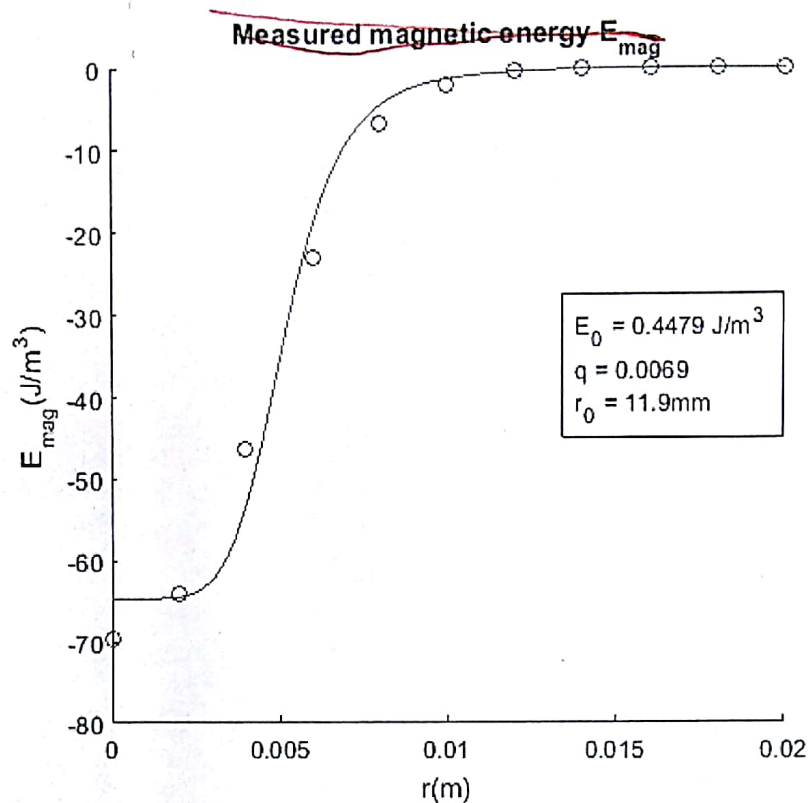


Figure 5: Measured magnetic energy around the magnet and its fit, including parameters of best fit.

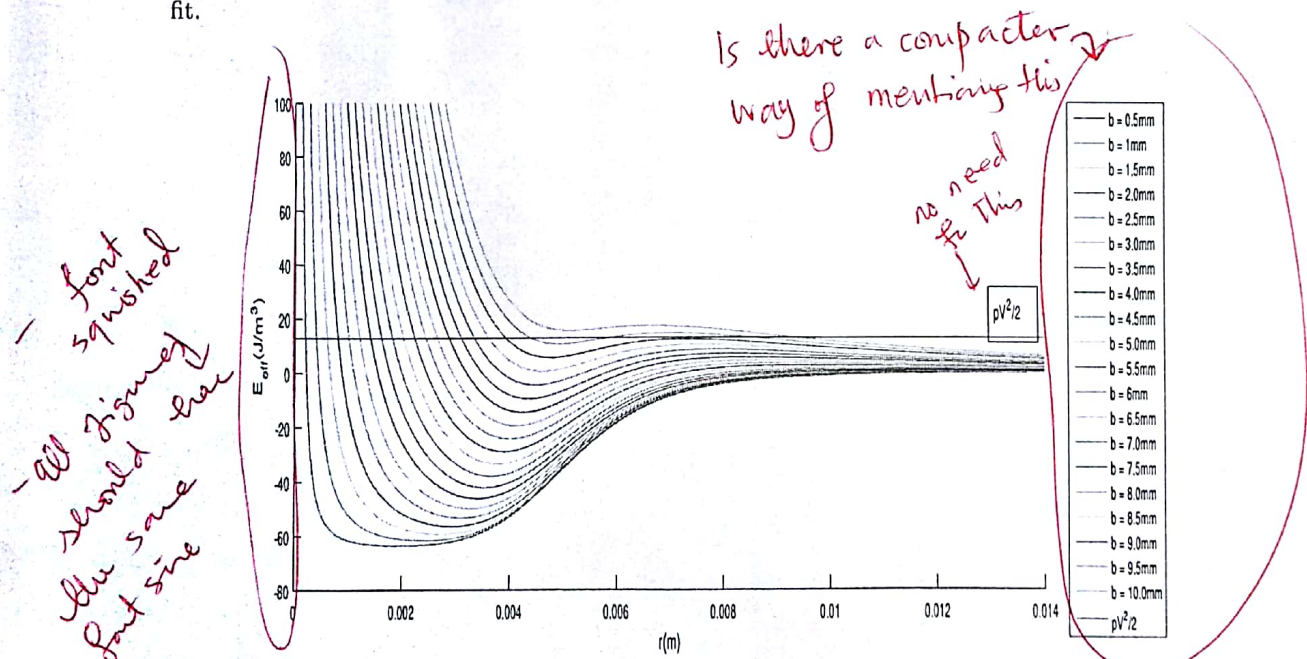


Figure 6: Effective magnetic energy  $E_{eff}$  per unit volume as a function of the drop-magnet distance  $r$ , for  $V = (17 \pm 2) \text{ cm/s}$  and different impact parameters  $b$ .

Likewise, (15) was solved by numerical integration and  $\alpha$  found for varying values of  $b$ . The resulting graph has been plotted in Fig. 8. Experimentally obtained values for  $\alpha$  using tracking software are shown on the same graph as circles.

From Fig. 7, it is seen that  $r_p$  is discontinuous at  $b \approx 8.7 \text{ mm}$ . In Fig. 7, a singular behaviour appears for this point as deflection seems to diverge. This represents the 'capture' situation, where drops were seen to orbit around the magnet. Looking at Fig. 6., this happens for approximately



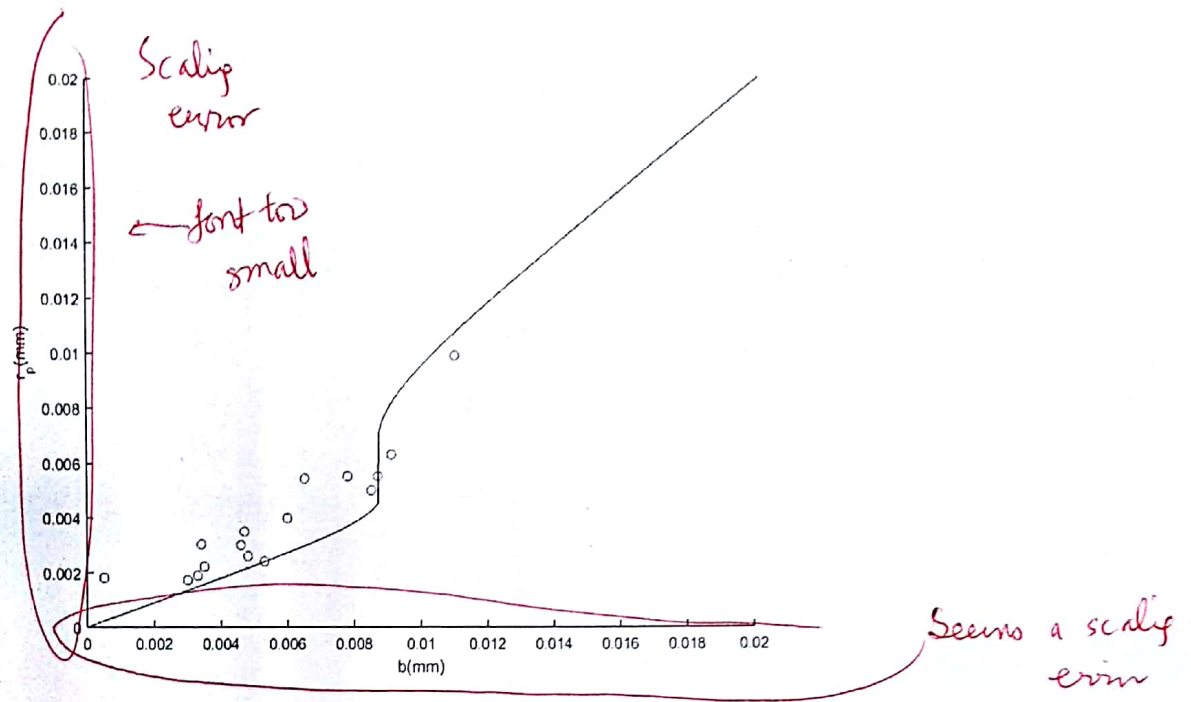


Figure 7: Distance  $r_p$  between the magnet and the pericenter of the trajectory as a function of  $b$ . The curve represents the model.

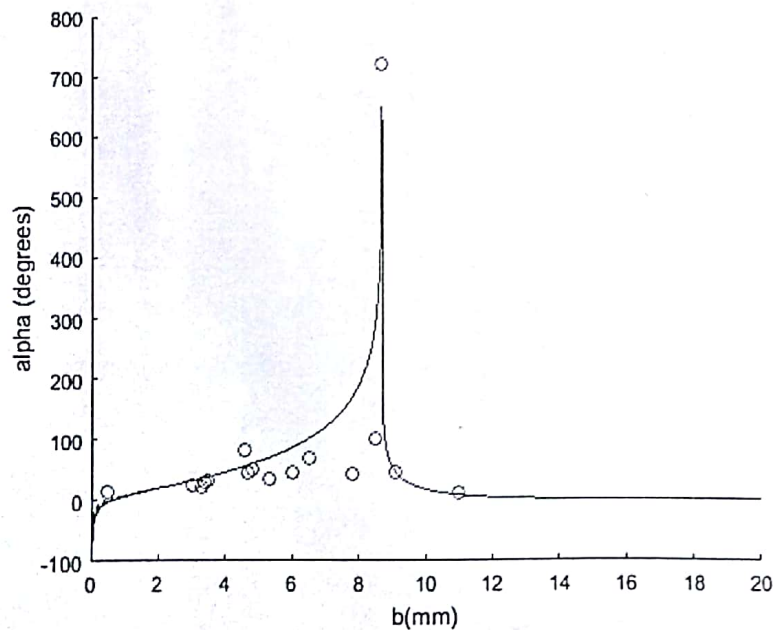


Figure 8: Angle of deflection  $\alpha$  as a function of  $b$  for  $V = (17 \pm 2)$  cm/s. The circles represent the experimentally measured values.

the same value of  $b$  ( $\approx 8.7$  mm) for which the pericenter is located on top of the local maximum of  $E_{eff}(r)$ . This corresponds to a point of unstable equilibrium; both the radial velocity and the radial acceleration are zero, hence the drop 'orbits' around the magnet (see Fig. 4. (b).)

## 6 Conclusion and Discussion

How

It has been previously shown that the topology of surfaces can be manipulated to induce self propelled motion of Leidenfrost drops [6]. We show that it is possible to alter trajectories of paramagnetic drops by the application of an external inhomogeneous magnetic field. This can have a range of applications where the control of small liquid droplets is important e.g. in thermal exchange, spray cooling, ink-jet printing, micro heat exchange in microchips etc.

However, there is sufficient room for improvement in the experimental design to probe further into a quantitative analysis. During video motion analysis it was observed that the drops were deformed when in close proximity of the magnet, resulting in energy dissipation. This effect needs to be taken into account while deriving the equation of motion. Experimental apparatus needs improvement too; while recording the video the aluminum rod was displaced by hand to vary the impact parameter, making the results very prone to human error. Instead of using a Plexiglas sheet, glass can be used with a grid printed on it to better adjust the impact parameter. As the drops were highly mobile, even small errors in estimates of the impact parameter resulted in very different trajectories, hence a better set up is needed to vary the impact parameter (Fig. 4.a) and as a result improve accuracy.

## References

- use a short code  
too long
- [1] <https://www.physlab.org/experiment/steering-paramagnetic-leidenfrost-drops-in-an-inhomogeneous-magnetic-field>
  - [2] Muhammad Sabieh Anwar Abdullah Irfan. Steering paramagnetic leidenfrost drops in an inhomogeneous magnetic field. — source ?
  - [3] J. Dewar. *Selected papers of Sir James Dewar*. Cambridge University Press. Year? place?
  - [4] Guillaume Dupeux, Marie Le Merrer, Christophe Clanet, and David Quéré. Trapping leidenfrost drops with crenulations. *Phys. Rev. Lett.*, 107:114503, Sep 2011.
  - [5] D.A. McQuarrie et al. *General Chemistry*. 2005. Year? publisher?
  - [6] H. Linke, B. J. Alemán, L. D. Melling, M. J. Taormina, M. J. Francis, C. C. Dow-Hygelund, V. Narayanan, R. P. Taylor, and A. Stout. Self-propelled leidenfrost droplets. *Phys. Rev. Lett.*, 96:154502, Apr 2006.